

## OCEANOGRAPHY

# A continuous pathway for fresh water along the East Greenland shelf

Nicholas P. Foukal<sup>1\*</sup>, Renske Gelderloos<sup>2</sup>, Robert S. Pickart<sup>1</sup>

**Export from the Arctic and meltwater from the Greenland Ice Sheet together form a southward-flowing coastal current along the East Greenland shelf. This current transports enough fresh water to substantially alter the large-scale circulation of the North Atlantic, yet the coastal current's origin and fate are poorly known due to our lack of knowledge concerning its north-south connectivity. Here, we demonstrate how the current negotiates the complex topography of Denmark Strait using in situ data and output from an ocean circulation model. We determine that the coastal current north of the strait supplies half of the transport to the coastal current south of the strait, while the other half is sourced from offshore via the shelfbreak jet, with little input from the Greenland Ice Sheet. These results indicate that there is a continuous pathway for Arctic-sourced fresh water along the entire East Greenland shelf from Fram Strait to Cape Farewell.**

## INTRODUCTION

Along the continental shelf of East Greenland, fresh water near the coast and saltier water offshore create a cross-shelf density gradient that supports a southward-flowing coastal current (Fig. 1A). The current intensifies as it flows southward, reaching a maximum of about 2 Sverdrups (Sv; 1 Sv =  $10^6$  m<sup>3</sup>/s) near Cape Farewell (1). Despite its relatively small transport, the exceptionally fresh waters of the East Greenland Coastal Current (EGCC) make it a vital component of the large-scale circulation. Over 30% of the total oceanic freshwater transport between Greenland and Scotland is carried by the EGCC [referenced to the section mean salinity (2)], and it is an important component of the Arctic freshwater budget (1).

As the EGCC rounds Cape Farewell, a portion of the fresh water progresses northward along the west coast of Greenland, while the remainder is fluxed offshore into the interior of the subpolar gyre (1). The potential fate of this fresh water in regions of deep water formation has led many to speculate that the accelerating melting of the Greenland Ice Sheet (3, 4) will stratify the subpolar gyre, slow or stop the Atlantic Meridional Overturning Circulation (AMOC) (5–7), and trigger nonlinear shifts in future climate sensitivity (8). However, the fresh water on the East Greenland shelf is also supplied by the Arctic via Fram Strait (9, 10), and the Arctic may play a larger role in setting the coastal current's variability than the input from Greenland (11, 12). This distinction between the two source regions is particularly important because fresh water stored in the Beaufort Gyre may be released in pulses when the anticyclonic winds periodically weaken (13), whereas input from the Greenland Ice Sheet will likely increase more gradually. The existence of a continuous pathway for the EGCC from Fram Strait to Cape Farewell will determine whether both sources of fresh water will primarily affect deep-water formation in the Greenland and Iceland Seas or continue southward into the North Atlantic and affect convection in the subpolar gyre.

Direct observations of the EGCC are plentiful south of Denmark Strait (1, 2, 11, 14–18), but the current's evolution north of 66°N is poorly known. A series of observational and theoretical papers

(17, 19) suggested that the EGCC could emerge from the interaction of the East Greenland Current with the deep Kangerdlugssuaq Trough. In this conceptual model, a net input of fresh water into the trough splits into the coastal current south of Denmark Strait and a return flow out of the trough. Although this model does not require a coastal current upstream of Denmark Strait, such a coastal current has been observed in the Nordic domain as far north as Fram Strait (20, 21), referred to as the Polar Surface Water Jet (21). This raises the question of whether the EGCC south of Denmark Strait is supplied by more northerly sources.

In this study, we use shipboard hydrographic data from multiple cruises, a high-resolution regional ocean circulation model, and historical surface drifters to address the connectivity of the coastal current across Denmark Strait. We find that while the coastal current does indeed connect across Denmark Strait, it is enhanced by flow diverted inshore from the shelfbreak north of the strait, with little input from the Greenland Ice Sheet. This onshore flow is due to both downwelling-favorable winds pushing fresh water closer to the coast and a geostrophic onshore flow induced by the widening of the shelf at Denmark Strait. This process may be broadly applicable to other buoyant coastal current systems. Last, surface drifter tracks along the East Greenland shelf demonstrate that the coastal current flows continuously from Fram Strait to Cape Farewell.

## RESULTS

### Role of the Kangerdlugssuaq Trough

We first examine the previous hypothesis that a net input of fresh water into the Kangerdlugssuaq Trough is the origin of the EGCC. In 2003, a section of expendable conductivity-temperature-depth (XCTD) casts and vessel-mounted acoustic Doppler current profiler (ADCP) measurements was taken at the mouth of the trough (Fig. 1B, red). Across this line (fig. S1), a clear inflow along the eastern boundary and outflow on the western boundary confirm the presumed geostrophic circulation (19, 22, 23). However, in contrast to expectations, the isohalines are deepest in the outflow on the western side of the trough, yielding a slight export of 0.04 Sv of waters fresher than 34 from the trough. To determine how representative this single snapshot is, we consult a 2-km resolution ocean circulation model of the region (see Materials and Methods for a full description

Copyright © 2020  
The Authors, some  
rights reserved;  
exclusive licensee  
American Association  
for the Advancement  
of Science. No claim to  
original U.S. Government  
Works. Distributed  
under a Creative  
Commons Attribution  
License 4.0 (CC BY).

<sup>1</sup>Woods Hole Oceanographic Institution, Woods Hole, MA 02543, USA. <sup>2</sup>Department of Earth and Planetary Sciences, The Johns Hopkins University, Baltimore, MD 21218, USA. \*Corresponding author. Email: nfoukal@whoi.edu

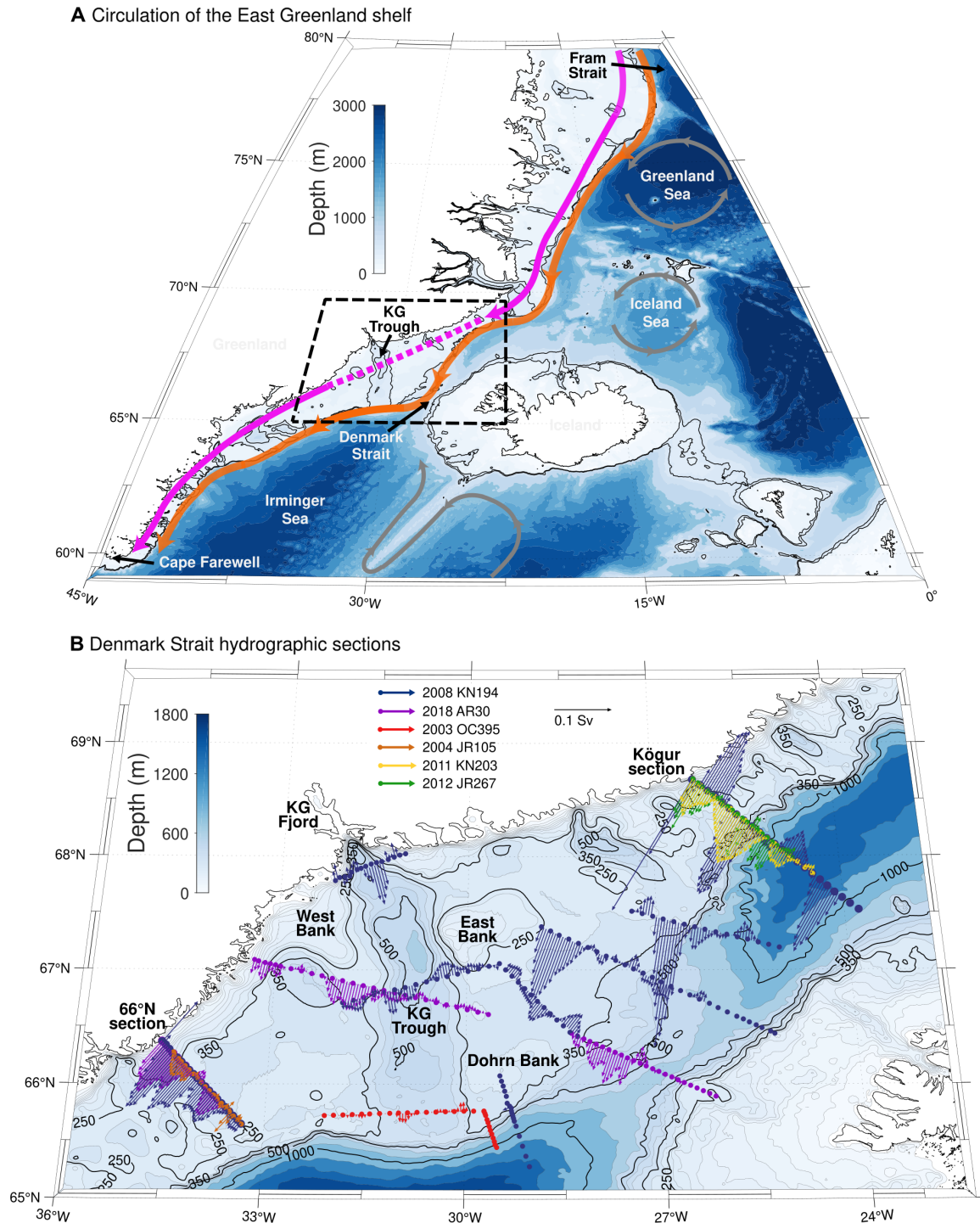


**Fig. 1. Circulation of the East Greenland shelf.** (A) Schematic circulation of the East Greenland shelf region. Bathymetry is shaded, and the 350- and 500-m isobaths are highlighted in black. The East Greenland Current (orange) flows southward at the shelfbreak along the entirety of East Greenland. The EGCC (pink) has been documented upstream of Denmark Strait and downstream of the Kangerdlugssuaq (KG) Trough, but its connection across Denmark Strait is unknown (dashed line). Other circulation features are shown in gray. The black dashed line outlines the region shown in (B). (B) Depth-integrated absolute geostrophic transports (see section S1) for water with salinity less than 34 from various hydrographic sections across Denmark Strait (year and cruise codes provided in legend). Bathymetric contours are shown every 25 m from 0 to 250 m, every 50 m for 250 to 500 m, and every 200 m deeper than 600 m. The 250-, 350-, 500-, and 1000-m isobaths are highlighted in black.

of the model setup). In the annual mean from the model, the freshest waters are likewise found on the western side of the trough, thereby leading to an export of fresh water regardless of the reference salinity. Given that this conceptual model requires a net import of fresh water to supply the coastal current, the EGCC does not appear to originate in the Kangerdlugssuaq Trough, motivating an analysis of the coastal current across Denmark Strait.

### Connectivity of the coastal current across Denmark Strait

To examine the presence of the coastal current as it enters Denmark Strait, we consider the salinity, density, and absolute geostrophic velocity at the Kögur hydrographic line between 68° and 69°N (Figs. 1B and 2). We use three occupations of the line that sampled to within 2 km of the coast between 2008 and 2012. The average conditions on the shelf during these three occupations compare well to the year-long model mean conditions extracted along the same line (Fig. 2). A narrow shelf (~60 km wide) brings the shelfbreak jet in close proximity to the coastal current and can make it difficult to differentiate between these currents instantaneously. To separate the currents and calculate their transports, we define all southward velocities on the

inner half of the shelf (0 to 30 km) fresher than 34 salinity as the coastal current (11, 14, 17). The transport of the simulated coastal current varies between 0 and 2 Sv and aligns well with the observed sections (Fig. 2E). From this analysis of the model and observations, we conclude that there is a persistent southward coastal current at the Kögur line that transports  $0.56 \pm 0.39$  Sv (model mean  $\pm 1$  SD) toward Denmark Strait.

At the southern end of our domain, we similarly quantify the coastal current using three shipboard occupations of a hydrographic line at 66°N, plus the model output (Figs. 1B and 3). Here, the wider shelf (~120 km) and more gently sloped bathymetry yield a broader coastal current; thus, we extend the offshore boundary to 50 km from the coast. The mean transport of the EGCC from the observations and simulation at 66°N is  $1.19 \pm 0.68$  Sv, over twice that at the Kögur line.

### Contribution of the shelfbreak jet to the EGCC

A doubling of the coastal current between Kögur and 66°N indicates that there is a convergence of fresh water onto the shelf between these locations, either from offshore via the shelfbreak jet or from onshore via Greenland meltwater. To identify locations where

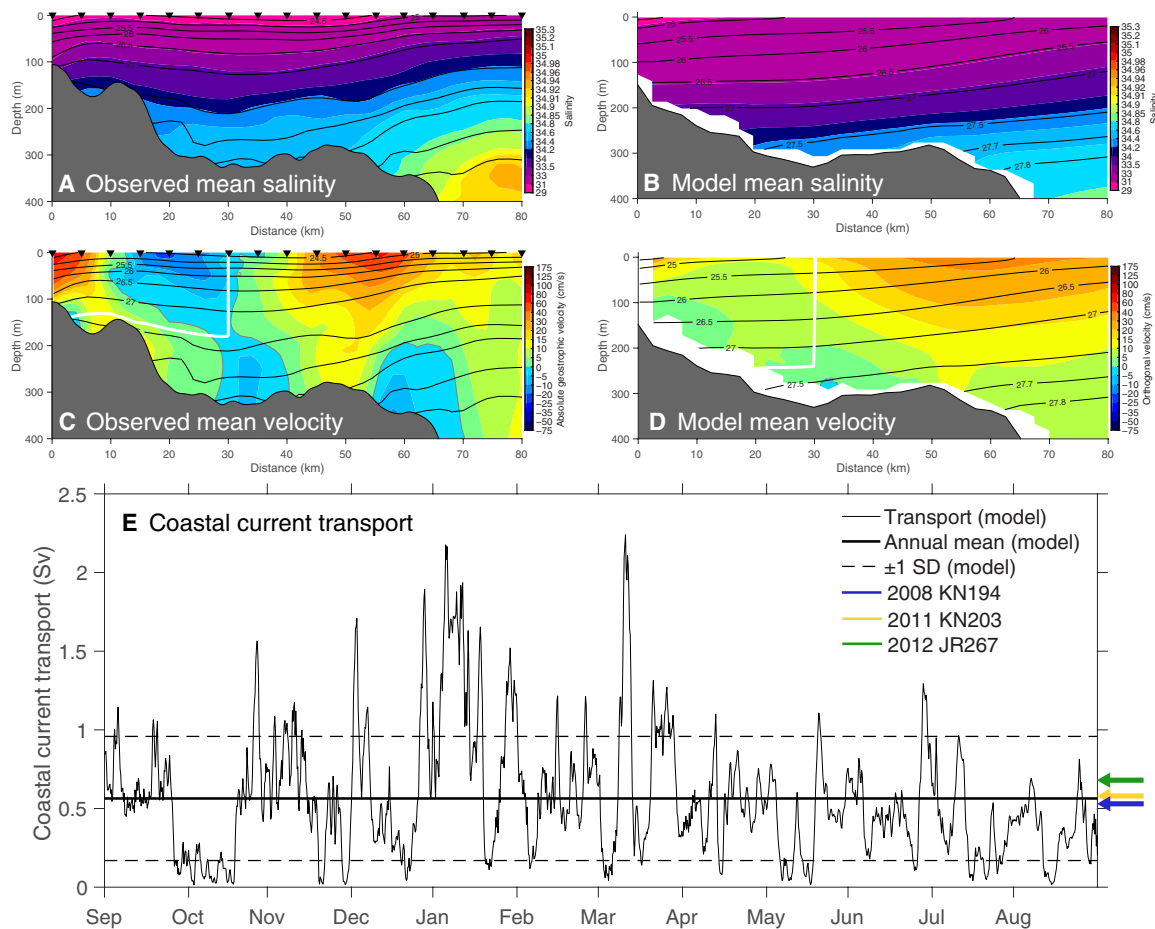


**Fig. 2. Observed and modeled hydrography at the Kögur line.** Salinity (A and B) and velocity (C and D) at the Kögur hydrographic line. The observed mean conditions (A and C) are averaged over three synoptic snapshots in October 2008 (KN194), August 2011 (KN203), and August 2012 (JR267). Black triangles above (A) and (C) indicate the typical 5-km spacing of CTD stations along the three transects. The model mean conditions (B and D) are averaged over the entire model year. In (A) to (D), isopycnals ( $\text{kg}/\text{m}^3$ ) are overlaid in black, and bathymetry is shaded in gray. Bounds of the coastal current (fresher than 34 salinity and between 0 and 30 km from the coast) are outlined in white in (C) and (D). Southward currents located between 40 and 80 km offshore are considered part of the shelfbreak jet. (E) Time series of the coastal current volume transport from the model. The observed transports calculated from the three snapshots are indicated by the arrows to the right of the plot.

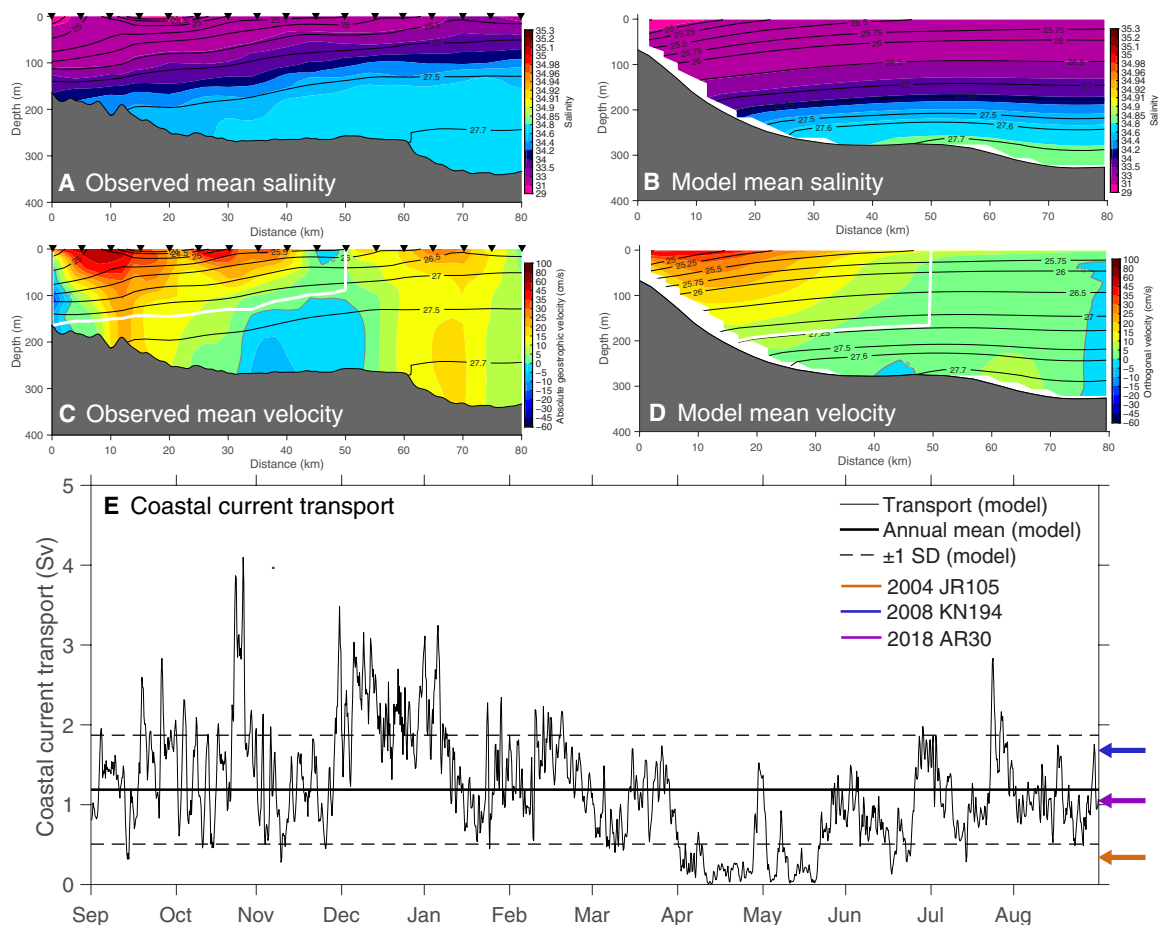


**Fig. 3. Observed and modeled hydrography at the 66°N line.** Salinity (A and B) and velocity (C and D) at the 66°N line. The observed mean conditions (A and C) are averaged over three synoptic snapshots in August 2004 (JR105), October 2008 (KN194), and October 2018 (AR30). KN194 and AR30 sampled to within 3 km of the coast, while JR105 ended 15 km from the coast. Black triangles above (A) and (C) indicate the typical 5-km spacing of CTD stations along the three transects. The model mean conditions (B and D) are averaged over the entire model year. In (A) to (D), isopycnals ( $\text{kg}/\text{m}^3$ ) are overlaid in black, and bathymetry is shaded in gray. Bounds of the coastal current (fresher than 34 salinity and between 0 and 50 km from the coast) are outlined in white in (C) and (D). (E) Time series of the coastal current volume transport from the model. The observed transports calculated from the three snapshots are indicated by the arrows to the right of the plot.

transport from the shelfbreak jet contributes to the coastal current intensification, we consider a region in the model enclosed by the Kögur section, the 66°N section, and two adjoining along-shelf sections inshore of the shelfbreak (Fig. 4). The calculated net transport of water fresher than 34 salinity across the southern along-shelf line (section 2 in Fig. 4A) is  $0.45 \pm 1.09$ , directed offshore. This is consistent with the observed net export across the 2003 XCTD section (OC395) at the mouth of the Kangerdlugssuaq Trough. The onshore convergence occurs farther north, where a net onshore (cross-isobath) flow of  $1.23 \pm 1.23$  Sv across section 3 in Fig. 4A explains the current's observed intensification.

To further diagnose this cross-isobath flow in the model, we seeded Lagrangian trajectories in the coastal current along the 66°N section and ran them backward in time to determine their origin (see Materials and Methods for a full description of the Lagrangian trajectories). The onshore transport is clearly evident in the Lagrangian pathways: Particles in the shelfbreak jet are deflected into the coastal current upstream of Dohrn Bank, and relatively few trajectories enter the Kangerdlugssuaq Trough at its mouth (color shading in Fig. 4A).

As this analysis only considers waters fresher than 34 salinity, there is the possibility that vertical mixing across the 34 isohaline could also affect the budgets. However, the sum of the horizontal Eulerian transports nearly closes (residual of 0.01 Sv), and fewer than 3% of the Lagrangian trajectories cross the 34 isohaline along their pathway in the domain. Therefore, we conclude that vertical mixing across the 34 isohaline on the shelf is limited and that the primary driver of the coastal current intensification is a horizontal convergence of fresh water across section 3 on the western side of Denmark Strait (Fig. 4A).

The majority (0.70 Sv of 1.23 Sv) of this onshore flow occurs in the Ekman layer (upper 40 m), and the variance of the Ekman layer flow is largely explained (60%) by the variance in the theoretical Ekman transport calculated using the along-section northerly winds (see section S2). Thus, the onshore convergence of fresh water can be explained primarily by local winds driving the fresh surface waters shoreward via a downwelling Ekman circulation. In addition to the downwelling-favorable Ekman circulation that induces an onshore flow of the upper-layer water and an offshore flow of lower-layer

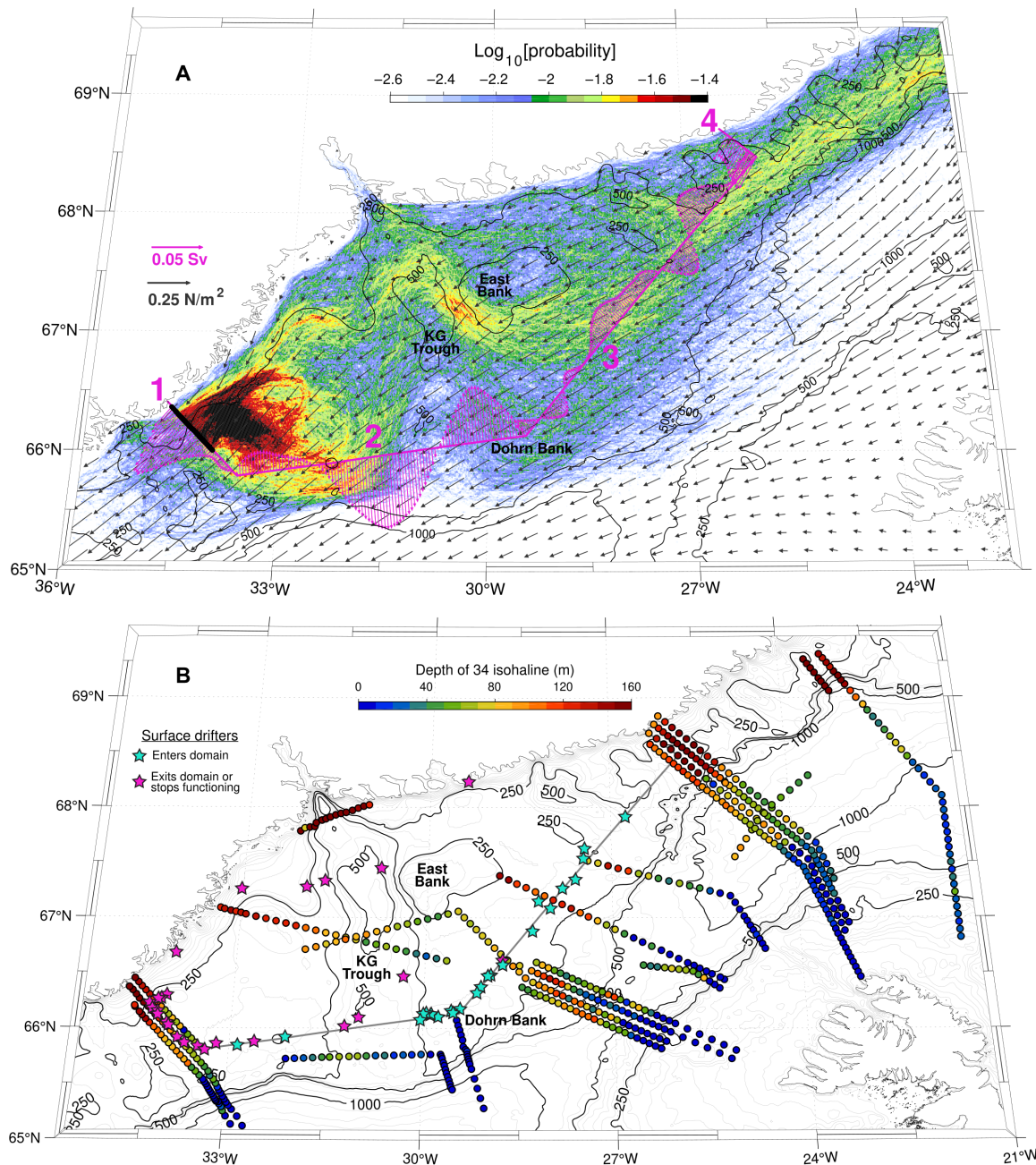


**Fig. 4. Modeled and observed pathways across Denmark Strait.** Fresh water pathways across Denmark Strait. (A) Modeled fresh water pathways from Eulerian and Lagrangian perspectives. Distribution of Lagrangian trajectories (color shading, note the log scale) seeded at the 66°N section (black circles) and run backward in time for 150 days (see section S3 for a full description of the Lagrangian trajectories). The Eulerian volume transports across model sections 1 to 4 for waters fresher than 34 salinity are shown by the magenta vectors. The time-averaged surface stress vectors are shown in black. (B) Observational evidence for fresh water convergence upstream of the Kangerdlugssuaq Trough. Depth of the 34 isohaline at various hydrographic sections (shaded circles). Sections that have been occupied multiple times are offset from one another for clarity. Surface drifter crossing locations as the drifters enter the domain (cyan stars) and leave the domain or stop functioning (magenta stars). Model sections 2 and 3 (gray line) constitute the seaward edge of the domain.

water, there is also a full-depth integrated onshore flow across section 3 (Fig. 4) of 0.86 Sv that cannot be explained by Ekman theory. This full-depth flow is sustained by an along-section density gradient, with denser water located at the southern end of the section near Dohrn Bank (fig. S2). The origin of this density gradient is also wind driven: The along-coast winds contain a slightly cross-sectional (or cross-isobath) component due to the local deviation between the

isobaths and the coastline, and this component of the wind pushes light waters toward the northern end of the section. The resulting Ekman setup yields a higher sea surface height at the Kögur line, supporting a geostrophic onshore flow. Thus, the along-coast, downwelling-favorable winds drive both an ageostrophic, downwelling-favorable Ekman circulation, and a geostrophic onshore flow due to the widening of the shelf north of Denmark Strait. Together, these

flows converge fresh water onto the shelf upstream of Denmark Strait and contribute to the coastal current's intensification.

To support this model-based result with observations, we consider the tracks of all 25 surface drifters (24) that crossed the domain over the 30-year period between 1989 and 2018 (Fig. 4B, stars). Although sparsely distributed, the surface drifters generally confirm the model's pathways of fresh water: 15 of the 25 drifters entered the domain between Dohrn Bank and the Kögur line, and 11 of the 18 that left the domain (7 stopped functioning on the shelf) exited across the 66°N section as part of the coastal current. Therefore, the majority of the surface drifters joined the coastal current from the shelfbreak jet upstream of Denmark Strait and then left across the 66°N section in the coastal current. In addition, we consider the depth of the 34 isohaline from historical hydrographic sections in the region as an indicator of the abundance of fresh water (Fig. 4B). As expected, the isohaline is deepest close to the coast and shoals offshore. Importantly, little to no fresh water is present near Dohrn Bank and the mouth of the Kangerdlugssuaq Trough, demonstrating that the fresh water accumulates on the shelf in Denmark Strait rather than circulates into the trough around Dohrn Bank.

### Contribution of Greenland meltwater to the EGCC

Our results demonstrate that the coastal current intensifies as it proceeds through the Denmark Strait region, and previous measurements show that the EGCC transport continues to increase as it flows to Cape Farewell (1). This latter observation has been traditionally used to argue that meltwater from the Greenland Ice Sheet contributes to the coastal current transport (14). We see possible evidence of meltwater in a hydrographic section from October 2008 at the mouth of Kangerdlugssuaq Fjord (see Fig. 1B), which drains the largest glacier in East Greenland. In this section, 0.25 Sv of water fresher than 34 is leaving the fjord, which is considerably larger than expected. In comparison, the freshwater input of the entire Greenland Ice Sheet is 40 mSv (25), of which the Kangerdlugssuaq Glacier accounts for about 5% (26). The Knudsen relation indicates that with a coastal current salinity of 33.5 (e.g., Fig. 3B), fresh runoff ( $S = 0$ ), and ambient ocean water ( $S = 35$ ), the effect of the glacial water on the coastal current transport should be ~20 times the discharge and runoff transport (27), which is similar to entrainment numbers calculated with noble gas tracers (28, 29). Thus, the Kangerdlugssuaq Fjord should contribute ~40 mSv to the coastal current, which is minimal compared to the coastal current's 1- to 2-Sv transport. The comparatively large outflow (0.25 Sv) captured in the 2008 section left the fjord in an anticyclonic upper-layer circulation pattern (30), suggesting that the hydrographic section might have captured an anticyclonic eddy or one phase of a coastally trapped wave. An analysis of the same section in the model confirms this: The section has essentially zero net export of fresh water in the mean, although 0.25 Sv is within the model's variability. Given the overall good agreement between the model and observations shown above, it is thus likely that the single hydrographic section captured the fjord in an intense outflow event rather than close to its mean state. We conclude that runoff from the Greenland Ice Sheet cannot explain the observed intensification of the coastal current through Denmark Strait.

### Pathways along the East Greenland shelf and shelfbreak

Both the EGCC (or Polar Surface Water Jet, which is what the coastal current is referred to north of Denmark Strait) and the East Greenland

Current (i.e., the shelfbreak jet) transport fresh water southward along the majority of Greenland's East Coast. Both currents are thus conduits for Arctic fresh water that could ultimately end up in the subpolar gyre. However, pathways of ice-mounted surface buoys from the International Arctic Buoy Program (31) demonstrate that floats in these currents meet different fates (Fig. 5). The buoys offshore of the 500-m isobath (seaward of the shelfbreak) are readily mixed offshore into the Greenland and Iceland Seas, while the buoys on the shelf progress more coherently southward through Denmark Strait into the subpolar North Atlantic. This is understandable in that the East Greenland Current is baroclinically unstable and readily forms

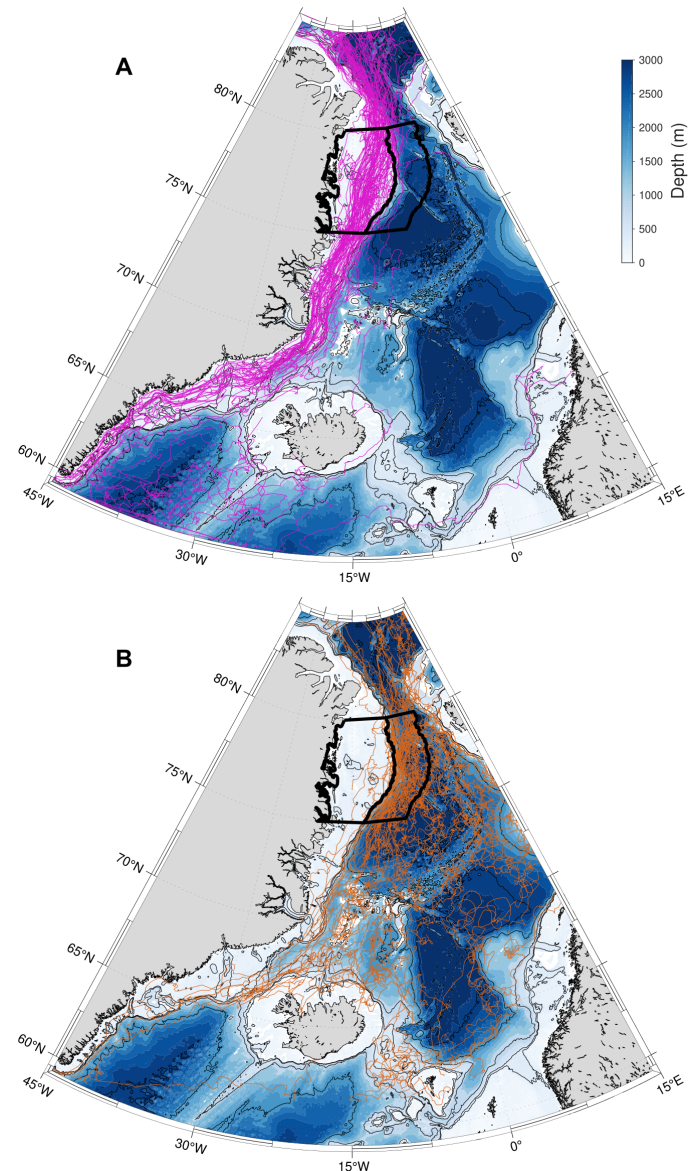


**Fig. 5. Observed surface circulation of the East Greenland shelf.** Trajectories of ice-mounted buoys from the International Arctic Buoy Program. (A) All 92 buoys that crossed the shelf region delimited by the western polygon in black. (B) All 59 buoys that crossed the region offshore of the 500-m isobath, delimited by the eastern polygon. While all the buoys shown here are initially ice mounted, they continue as surface drifters once the ice around them melts.

eddies (21, 32). Its close proximity to the Greenland and Iceland Sea gyres means that this turbulent exchange will result in entrainment of fresh water into the gyres. In addition, there are several bifurcation points along the path of the East Greenland Current—including where the Jan Mayen Current forms (33) and where the East Icelandic Current forms (34)—which lead to an advective offshore flux. By contrast, the coastal current remains largely isolated from energetic shelfbreak processes and, thus, serves as a direct route for fresh water to flow from the Arctic into the Irminger Sea.

## DISCUSSION

In this study, we have used observations and a numerical model to demonstrate that the EGCC connects across Denmark Strait; hence, the existence of the current south of the strait is not entirely locally sourced as previously hypothesized. We showed further that the current intensifies as it flows through the strait, gaining fresh water primarily from the offshore shelfbreak jet rather than input from the Greenland Ice Sheet. Analysis of historical ice drifters revealed that, while the coastal current represents a coherent pathway from Fram Strait into the Irminger Sea, water in the shelfbreak jet more readily enters the interior of the Nordic Seas.

Our results suggest that Arctic-sourced fresh water will be more apt to affect and modulate convection in the Nordic Seas if the fresh water exits Fram Strait via the shelfbreak jet. By contrast, fresh water leaving the Arctic in the coastal current, along with glacial meltwater, is more readily able to enter the North Atlantic Ocean, where it could influence convection in the subpolar gyre.

It has recently been demonstrated that the Greenland Sea is the source of the densest component of the AMOC (35). On the other hand, open-ocean convection in the Labrador and Irminger Seas feeds the intermediate branch of the AMOC. Hence, the coastal current and shelfbreak jet, although flowing side by side, have the ability to influence the climate system in very different ways. Much has been made of the potential impact on the AMOC due to the melting of the Greenland Ice Sheet (5–7), or the release of fresh water from the Beaufort Gyre (13). Our results imply that, to determine the AMOC response to this increased fresh water, an improved understanding of the pathways and detailed dynamics of the coastal circulation east of Greenland is required.

## MATERIALS AND METHODS

### Absolute geostrophic velocity from hydrographic sections

To calculate the absolute geostrophic velocity sections shown in Figs. 2B and 3B and fig. S1B, we first interpolate the potential temperature and salinity data measured at the individual conductivity-temperature-depth (CTD) stations onto a standard grid with 2-km horizontal spacing and 10-m vertical spacing. From these sections, we derive the potential density and then calculate a relative geostrophic shear profile using the thermal wind relation. To reference the geostrophic shear to an absolute velocity, we calculate a reference velocity for each location along the section. We do this by vertically averaging the shipboard ADCP data across the section to remove noise from the shipboard ADCP data. We then reference the geostrophic shear to the vertical midpoint of the ADCP data. The resulting absolute geostrophic velocity is a dynamically consistent velocity profile that is referenced to directly measured current velocities.

## Description of the MITgcm model setup

The ocean circulation model used in this work is a high-resolution configuration of the Massachusetts Institute of Technology general circulation model (MITgcm) (36), identical to the setup in Almansi *et al.* (37), except for the atmospheric forcing that is provided by the Arctic System Reanalysis. The model is run for the period 1 September 2007 to 31 August 2008, and model output is saved at 6-hourly resolution. The full model domain is 56.8° to 76.5°N, 46.9°W to 1.3°E, with 2-km horizontal resolution in the region of interest and 216 vertical levels. Model boundary conditions are obtained from the 1/12° Hybrid Coordinate Ocean Model (HYCOM) with the Navy Coupled Ocean Data Assimilation (NCODA) for the ocean and from TOPAZv4 for sea ice. The model uses bathymetry from IBCAOv3 north of 64°N (i.e., our domain) and data from deep-diving seals. Surface runoff and solid ice discharge from Greenland are incorporated into the model forcings by adding water volume at the surface distributed over grid points near the glaciers as well as time-varying full-water column restoring of temperature and salinity at these grid points to account for plume entrainment. This model has been shown to accurately simulate the circulation in the Denmark Strait region (22, 37, 38). Model-based quantities have been extracted and calculated using OceanSpy (39).

## Lagrangian trajectories

Particles were seeded in the numerical model at the 66°N section in waters fresher than 34 salinity and within 50 km of the coast. The trajectories were run backward in time for 150 days. To determine how long the particles should be run, we conducted a 300-day test run. The number of particles in the domain flattens considerably after 150 days; thus, a longer integration time does not yield dramatically different results and also reduces the number of possible launches. We then seeded the particles on the last day of the month from February to August of 2008 (yielding seven launches total) and ran them backward in time for 150 days. In total, 2395 particles were released and were advected offline in the model's velocity field. Details on the calculation of the particle trajectories are given in Koszalka *et al.* (38) and Gelderloos *et al.* (40).

## SUPPLEMENTARY MATERIALS

Supplementary material for this article is available at <http://advances.sciencemag.org/cgi/content/full/6/43/eabc4254/DC1>

## REFERENCES AND NOTES

1. P. Lin, R. S. Pickart, D. J. Torres, A. Pacini, Evolution of the freshwater coastal current at the southern tip of Greenland. *J. Phys. Oceanogr.* **48**, 2127–2140 (2018).
2. I. A. A. Le Bras, F. Straneo, J. Holte, N. P. Holliday, Seasonality of freshwater in the East Greenland current system from 2014 to 2016. *J. Geophys. Res. Ocean.* **123**, 8828–8848 (2018).
3. F. Straneo, P. Heimbach, North Atlantic warming and the retreat of Greenland's outlet glaciers. *Nature* **504**, 36–43 (2013).
4. L. D. Trusel, S. B. Das, M. B. Osman, M. J. Evans, B. E. Smith, X. Fettweis, J. R. McConnell, B. P. Y. Noël, M. R. van den Broeke, Nonlinear rise in Greenland runoff in response to post-industrial Arctic warming. *Nature* **564**, 104–108 (2018).
5. S. Rahmstorf, J. E. Box, G. Feulner, M. E. Mann, A. Robinson, S. Rutherford, E. J. Schaffernicht, Exceptional twentieth-century slowdown in Atlantic Ocean overturning circulation. *Nat. Clim. Chang.* **5**, 475–480 (2015).
6. L. Caesar, S. Rahmstorf, A. Robinson, G. Feulner, V. Saba, Observed fingerprint of a weakening Atlantic Ocean overturning circulation. *Nature* **556**, 191–196 (2018).
7. D. J. R. Thornalley, W. Delia, P. Ortega, J. I. Robson, C. M. Brierley, R. Davis, I. R. Hall, P. Moffa-sanchez, N. L. Rose, P. T. Spooner, I. Yashayaev, L. D. Keigwin, Anomalous weak Labrador Sea convection and Atlantic overturning during the past 150 years. *Nature* **556**, 227–230 (2018).
8. A. Y. Glikson, North Atlantic and sub-Antarctic Ocean temperatures: Possible onset of a transient stadial cooling stage. *Clim. Change* **155**, 311–321 (2019).

9. L. de Steur, E. Hansen, R. Gerdes, M. Karcher, E. Fahrbach, J. Holfort, Freshwater fluxes in the East Greenland Current: A decade of observations. *Geophys. Res. Lett.* **36**, 2–6 (2009).
10. B. Rabe, P. A. Dodd, E. Hansen, E. Falck, U. Schauer, A. MacKensen, A. Beszczynska-Möller, G. Kattner, E. J. Rohling, K. Cox, Liquid export of Arctic freshwater components through the Fram Strait 1998–2011. *Ocean Sci.* **9**, 91–109 (2013).
11. B. E. Harden, F. Straneo, D. A. Sutherland, Moored observations of synoptic and seasonal variability in the East Greenland Coastal Current. *J. Geophys. Res. Ocean* **119**, 8838–8857 (2014).
12. L. de Steur, R. S. Pickart, A. Macrander, K. Våge, B. Harden, S. Jónsson, S. Østerhus, H. Valdimarsson, Liquid freshwater transport estimates from the East Greenland Current based on continuous measurements north of Denmark Strait. *J. Geophys. Res. Ocean* **122**, 83–109 (2017).
13. A. Proshutinsky, D. Dukhovskoy, M. L. Timmermans, R. Krishfield, J. L. Bamber, Arctic circulation regimes. *Philos. Trans. R. Soc. A Math. Phys. Eng. Sci.* **373**, 20140160 (2015).
14. S. Bacon, G. Reverdin, I. G. Rigor, H. M. Snaith, A freshwater jet on the East Greenland shelf. *J. Geophys. Res. Ocean* **107**, 5.1–5.16 (2002).
15. S. Bacon, A. Marshall, N. P. Holliday, Y. Aksenov, S. R. Dye, Seasonal variability of the East Greenland Coastal Current. *J. Geophys. Res. Ocean* 2121–2128 (2014).
16. R. S. Pickart, D. J. Torres, P. S. Fratantoni, The East Greenland Spill Jet. *J. Phys. Oceanogr.* **35**, 1037–1053 (2005).
17. D. A. Sutherland, R. S. Pickart, The East Greenland coastal current: Structure, variability, and forcing. *Prog. Oceanogr.* **78**, 58–77 (2008).
18. D. Wilkinson, S. Bacon, The spatial and temporal variability of the East Greenland Coastal Current from historic data. *Geophys. Res. Lett.* **32**, 10.1029/2005GL024232, (2005).
19. D. A. Sutherland, C. Cenedese, Laboratory experiments on the interaction of a buoyant coastal current with a canyon: Application to the East Greenland Current. *J. Phys. Oceanogr.* **39**, 1258–1271 (2009).
20. J. Nilsson, G. Björk, B. Rudels, P. Winsor, D. Torres, Liquid freshwater transport and Polar Surface Water characteristics in the East Greenland Current during the AO-02 Oden expedition. *Prog. Oceanogr.* **78**, 45–57 (2008).
21. L. Håvik, R. S. Pickart, K. Våge, D. J. Torres, A. M. Thurnherr, A. Beszczynska-Möller, W. Walczowski, W.-J. von Appen, Evolution of the East Greenland Current from Fram Strait to Denmark Strait: Synoptic measurements from summer 2012. *J. Geophys. Res. Ocean.* **122**, 2017–2033 (2017).
22. R. Gelderloos, T. W. N. Haine, I. M. Koszalka, M. G. Magaldi, Seasonal variability in warm-water inflow toward Kangerdlugssuaq Fjord. *J. Phys. Oceanogr.* **47**, 1685–1699 (2017).
23. N. J. Fraser, M. E. Inall, M. G. Magaldi, T. W. N. Haine, S. C. Jones, Wintertime Fjord-shelf interaction and ice sheet melting in Southeast Greenland. *J. Geophys. Res. Ocean.* **123**, 9156–9177 (2018).
24. R. Lumpkin, G. C. Johnson, Global ocean surface velocities from drifters: Mean, variance, El Niño–Southern Oscillation response, and seasonal cycle. *J. Geophys. Res. Ocean* **118**, 2992–3006 (2013).
25. J. L. Bamber, A. J. Tedstone, M. D. King, I. M. Howat, E. M. Enderlin, M. R. van den Broeke, B. Noel, Land ice freshwater budget of the Arctic and North Atlantic Oceans: 1. Data, methods, and results. *J. Geophys. Res. Ocean* **123**, 1827–1837 (2018).
26. E. M. Enderlin, I. M. Howat, S. Jeong, M. J. Noh, J. H. Van Angelen, M. R. Van Den Broeke, An improved mass budget for the Greenland ice sheet. *Geophys. Res. Lett.* **41**, 866–872 (2014).
27. P. MacCready, W. R. Geyer, Advances in Estuarine Physics. *Ann. Rev. Mar. Sci.* **2**, 35–58 (2010).
28. N. L. Beard, F. Straneo, W. Jenkins, Export of strongly diluted greenland meltwater from a Major Glacial Fjord. *Geophys. Res. Lett.* **45**, 4163–4170 (2018).
29. N. Beard, F. Straneo, W. Jenkins, Spreading of Greenland meltwaters in the ocean revealed by noble gases. *Geophys. Res. Lett.* **42**, 7705–7713 (2015).
30. D. A. Sutherland, F. Straneo, R. S. Pickart, Characteristics and dynamics of two major Greenland glacial fjords. *J. Geophys. Res. Ocean* **119**, 3767–3791 (2014).
31. I. G. Rigor, J. M. Wallace, R. L. Colony, Response of sea ice to the Arctic Oscillation. *J. Climate* **15**, 2648–2663 (2002).
32. K. Våge, R. S. Pickart, M. A. Spall, G. W. K. Moore, H. Valdimarsson, D. J. Torres, S. Y. Erofeeva, J. E. Ø. Nilsen, Revised circulation scheme north of the Denmark Strait. *Deep. Res. Part I Oceanogr. Res. Pap.* **79**, 20–39 (2013).
33. R. H. Bourke, R. G. Paquette, R. F. Blythe, The Jan Mayen current of the Greenland Sea. *J. Geophys. Res.* **97**, 7241 (1992).
34. A. Macrander, H. Valdimarsson, S. Jónsson, Improved transport estimate of the East Icelandic Current 2002–2012. *J. Geophys. Res. Ocean* 10.1002/2013JC009517, (2014).
35. S. Semper, K. Våge, R. S. Pickart, H. Valdimarsson, D. J. Torres, S. Jónsson, The emergence of the north icelandic jet and its evolution from northeast Iceland to Denmark strait. *J. Phys. Oceanogr.* **49**, 2499–2521 (2019).
36. J. Marshall, A. Adcroft, C. Hill, L. Perelman, C. Heisey, A finite-volume, incompressible navier stokes model for, studies of the ocean on parallel computers. *J. Geophys. Res. Ocean.* **102**, 5753–5766 (1997).
37. M. Almans, T. W. N. Haine, R. S. Pickart, M. G. Magaldi, R. Gelderloos, D. Mastropole, High-frequency variability in the circulation and hydrography of the Denmark strait overflow from a high-resolution numerical model. *J. Phys. Oceanogr.* **47**, 2999–3013 (2017).
38. I. M. Koszalka, T. W. N. Haine, M. G. Magaldi, Fates and travel times of Denmark strait overflow water in the Irminger Basin. *J. Phys. Oceanogr.* **43**, 2611–2628 (2013).
39. M. Almans, R. Gelderloos, T. Haine, A. Saberi, A. Siddiqui, OceanSpy: A Python package to facilitate ocean model data analysis and visualization. *J. Open Source Softw.* **4**, 1506 (2019).
40. R. Gelderloos, A. S. Szalay, T. W. N. Haine, G. Lemson, A fast algorithm for neutrally-buoyant Lagrangian particles in numerical ocean modeling. *e-Science* **2016**, 381–388 (2016).

**Acknowledgments:** We are grateful to the captains, crew, and scientists who sailed on the vessels that collected the hydrographic data used in this study. **Funding:** Funding for this work comes from the NSF under grant numbers OCE-1756361 and OCE-1558742 (N.P.F. and R.S.P.) and grant numbers OCE-1756863 and OAC-1835640 (R.G.). **Author contributions:** N.P.F. analyzed the in situ data and wrote the manuscript. R.G. analyzed the model data, ran the Lagrangian simulations, and contributed to the writing of the manuscript. R.S.P. devised the study and contributed to the writing of the manuscript. **Competing interests:** The authors declare that they have no competing interests. **Data and materials availability:** Hydrographic data used in this study are available at <https://rpickart.who.edu/research-projects/>. Model data used in this study are publicly available on SciServer (<http://sciserver.org>). The global surface drifter program data are available at [www.aoml.noaa.gov/phod/gdp/](http://www.aoml.noaa.gov/phod/gdp/). The International Arctic Buoy Program data are available at <http://iabp.apl.washington.edu/>.

Submitted 23 April 2020  
Accepted 26 August 2020  
Published 21 October 2020  
10.1126/sciadv.abc4254

**Citation:** N. P. Foukal, R. Gelderloos, R. S. Pickart, A continuous pathway for fresh water along the East Greenland shelf. *Sci. Adv.* **6**, eabc4254 (2020).



## A continuous pathway for fresh water along the East Greenland shelf

Nicholas P. Foukal, Renske Gelderloos and Robert S. Pickart

*Sci Adv* 6 (43), eabc4254.

DOI: 10.1126/sciadv.abc4254

### ARTICLE TOOLS

<http://advances.sciencemag.org/content/6/43/eabc4254>

### SUPPLEMENTARY MATERIALS

<http://advances.sciencemag.org/content/suppl/2020/10/19/6.43.eabc4254.DC1>

### REFERENCES

This article cites 37 articles, 0 of which you can access for free  
<http://advances.sciencemag.org/content/6/43/eabc4254#BIBL>

### PERMISSIONS

<http://www.sciencemag.org/help/reprints-and-permissions>

Use of this article is subject to the [Terms of Service](#)

---

*Science Advances* (ISSN 2375-2548) is published by the American Association for the Advancement of Science, 1200 New York Avenue NW, Washington, DC 20005. The title *Science Advances* is a registered trademark of AAAS.

Copyright © 2020 The Authors, some rights reserved; exclusive licensee American Association for the Advancement of Science. No claim to original U.S. Government Works. Distributed under a Creative Commons Attribution License 4.0 (CC BY).